DUST EMISSION FROM BARNARD 35: GAS HEATING ANOMALY RESOLVED

Howard A. Smith
Naval Research Laboratory
Washington, D.C. 20375

ABSTRACT

The molecular cloud B35 has puzzled observers because it contains gas which is at $T_g \approx 23K$, hotter than the surrounding dust whose $T_d \approx 10K$. An investigation of the IRAS data, however, shows a previously unreported dust component at $T_d \approx 33K$ whose luminosity is ample to heat the gas. IRAS also finds that about 12% of the total luminosity around the core, and about 20% along the rim, arises from the small grain component with T≤300K. The temperatures of these two components vary across the source, and this behavior is discussed. The results illustrate the presence of multiple components of dust in these clouds, and emphasize the need for data at multiple wavelengths.

1. INTRODUCTION

Barnard 35 is a bright-rimmed dark cloud, one of a ring of such clouds located at the edge of the large HII region excited by the λ Ori OB association. It is about 18'x4' in overall size, and has a far infrared point source at the densest part of the cloud, at the western edge close to the bright rim. It has gas and dust temperatures that resemble in general those in other dark clouds and globules. Along the bright ridge, however, the CO is heated to $T_g = 23.4 \pm 3.5$ K, while measurements of the dust temperature in this ridge give $T_d = 10 \pm 5$ K (Lada et al., 1981). Because the usual model for gas heating uses gas-dust collisions, alternative mechanisms for heating the dust in this cloud have been investigated, but found inadequate or inconclusive. These including shock heating, magnetic viscous heating, and heating from the nearby star FU Ori (Lada and Wilking, 1980; Smith et al., 1982).

2. IRAS DATA

We have used the IRAS coadded data on B35 to analyze the emission from dust in three zones: the outer rim of the cloud, the small inner core along the line-of-sight to the embedded star, and the intervening region ("limb") between the two. Figure 1 shows the 60 μm IRAS image

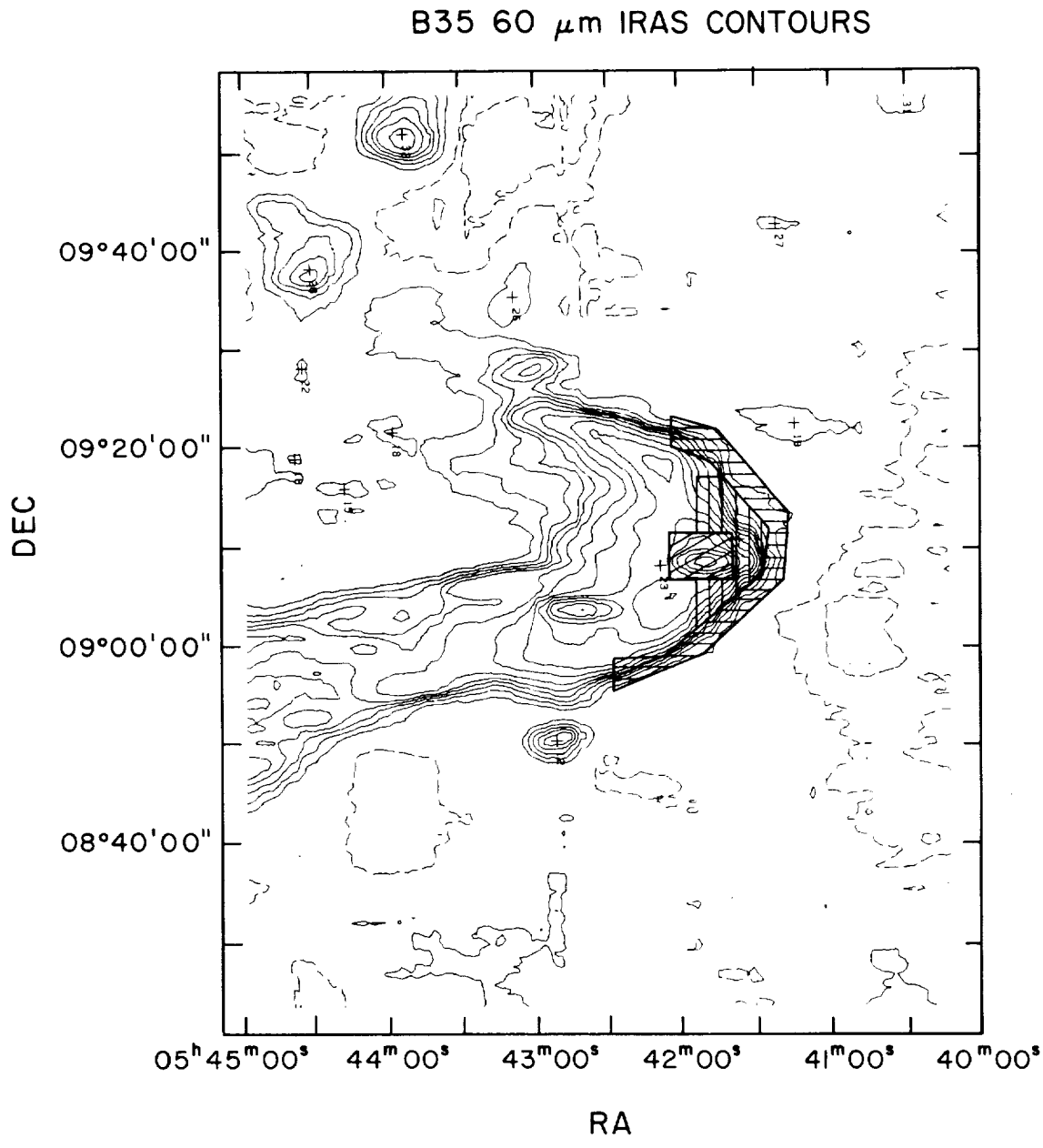

Figure 1: The IRAS 60 μm contours of the B35 cloud, with coordinates for epoch 1950.0. The three areas used for dust analysis (see text) are shown.

of B35, with the three zones indicated. The data reduction procedure first approximately corrected for overlying zodiacal emission by measuring the background at several locations away from the source, fitting that emission to a plane, and subtracting the plane from the entire image, at all four IRAS bands. Next the 12, 25 and 60 μm images were degraded to the same resolution as the 100 μm image, so that approximately equivalent areas were being compared; in each wavelength band the area examined was the same to within 5%. The AIPS software package was then used to measure the integrated intensity in each of the areas, in each of the bands, and the corresponding statistics. Next the data were color-corrected according to standard procedures as described in the IRAS Explanatory Supplement (Beichman et al., 1985). Finally the flux values were fit to a two temperature greybody model, whose emissivity was also varied according to υ^{β} with β=0, 1 or 2. Table 1 lists the results of this data reduction.

3. DISCUSSION

The data of Lada et al. were obtained from the Kuiper Airborne Observatory with a set of four far infrared filters, 80 μm being the shortest wavelength passed by the filters and diffraction limiting the long wavelength response. As a result the KAO system was very sensitive to the cold dust ($T_g \approx 10K$), which emits at wavelengths longer than about 140 μm, but was not sensitive to a warm component which IRAS easily detects. On the other hand the IRAS 100 μm filter passes very little radiation longward of about 110 μm

The IRAS data on B35 in fact reveal a warm 33K dust component not seen by the Lada et al. KAO observations. Figure 2 is a plot of the continuum emission from the 2′ region around the core, showing both the IRAS data and those from the KAO. The two data sets are mutually consistent because at IRAS wavelengths the flux from a λ^{-1} cold greybody is on the modified Wien tail and in this case down by a factor of 16 from the KAO data point. IRAS and KAO data each sample a different component of the dust. IRAS finds the luminosity in the ≈30K dust component around the core to be about 3.4 $L_{\odot}$, and over the entire region of warm CO gas about 700$L_{\odot}$, more than enough to provide the necessary gas heating and an order-of-magnitude larger than the previous estimates of cloud luminosity (Lada et al., 1981). We expect that multiple dust temperature components are the norm in dark clouds, and CO temperatures can provide a clue that warmer dust is present than is indicated by the data longward of 100 μm. The results emphasize the importance of observations at multiple wavelengths.

The IRAS data also show a strong component of high temperature emission, the small grain contribution, at a characteristic temperature of $\leq$ 300K, and cooling noticeably as the line-of-sight moves from the edge to the core of the cloud. The total luminosity in this high

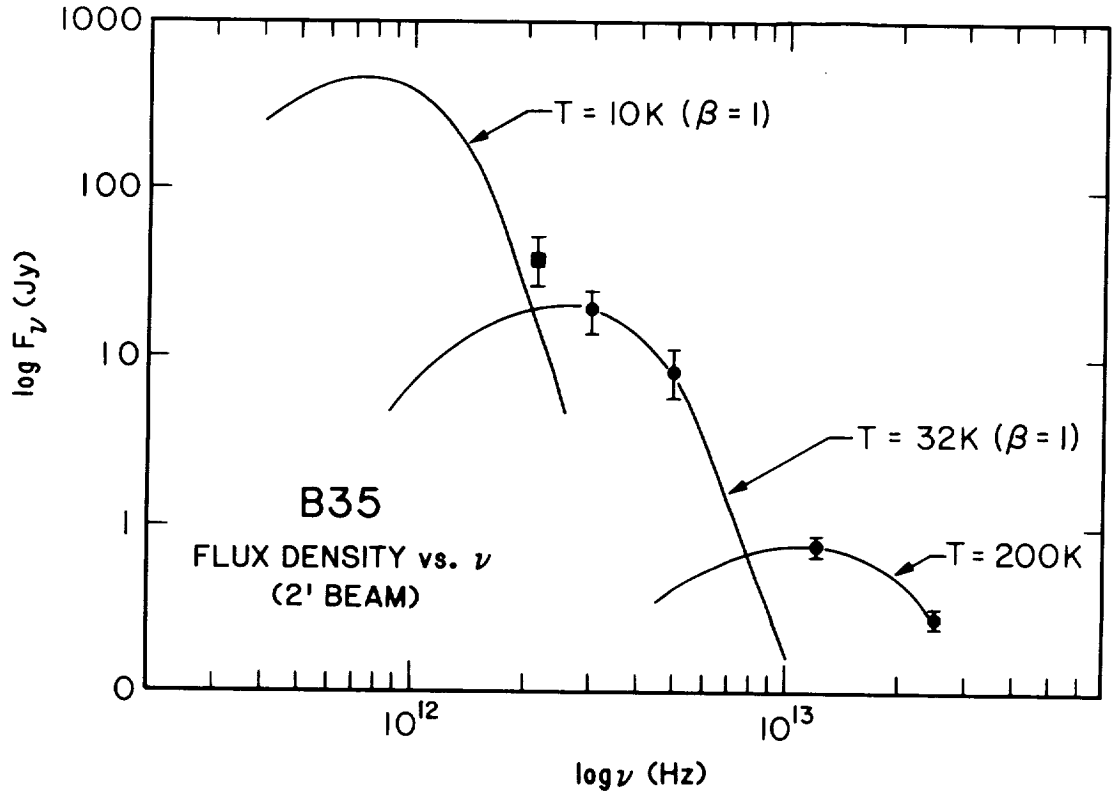

Figure 2: The continuum spectrum of B35 in a 2′ region around the core. The dots are from IRAS data, and the square from the KAO data of Lada et al. (1981). Curves are best fits to the data points, with assumed dust emissivity laws as indicated. The KAO data were obtained with a set of four long-wavelength pass filters, and the shape of the T=10K curve is determined by more data than this single point.

temperature component is between 10-20% of the total source luminosity, an amount comparable to that seen in other clouds. The low temperature component is at about 30K, and warms noticeable as the line-of-sight moves inward, behavior expected because of the presence of the embedded hot young star. Figure 3 plots the temperatures of these two components versus sampled area as the line-of-sight moves inward from the rim toward the cloud core. The optical depth of the dust at 100 μm in each of the three zones is $\approx 10^{-4}$.

The small grain component might itself contribute to the heating of the gas since its temperature and luminosity are more than ample. However the usual gas heating mechanism is collisional, and proportional to n_{gr}(hot)σ_{gr} n_{gr} (Burke and Hollenbach, 1983). The total abundance of small grains is estimated at $<10^{-2}$ by mass of the total dust (Sellgren, 1983), with the amount being hot at any time given approximately by the ratio of the cooling time to the time

between collisions, $\approx 10^{-2}$ (Dwek, 1984; private communication). In addition their geometrical cross-section is 4-5 orders-of-magnitude smaller than that of the normal dust component. If these grains are to heat the gas significantly, therefore, it must be through some more efficient mechanism, perhaps involving photoelectric heating (Draine and Sutin, 1987).

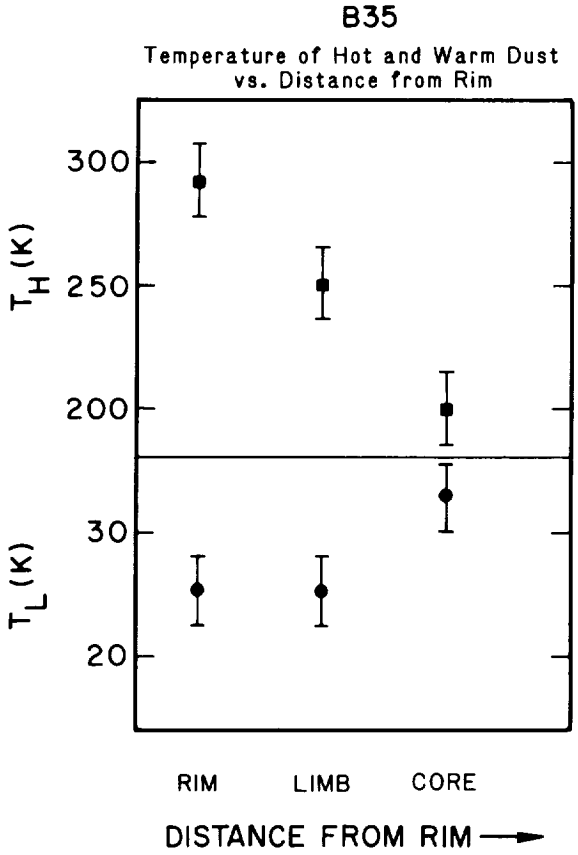

Figure 3: Plot of the temperature of the hot and warm dust components versus distance from the cloud rim. The uncertainties reflect both statistical flux errors and uncertainties in the appropriate spectral shape to use for color corrections and temperature fitting. All data are from the IRAS coadded scans.

REFERENCES

Beichman, C.A., Neugebauer, G., Habing, H.J., Clegg, P.E., and Chester, T.J.: 1985, *IRAS Catalogs and Atlases Explanatory Supplement* (Pasadena, JPL)

Burke, J.R. and Hollenbach, D.J.: 1983, Ap.J., 265, 223

Draine, B.T. and Sutin, B.: 1987, Ap.J., 320, 803

Dwek, E: 1986, Ap.J., 302, 363

Lada, C.J. and Wilking, B.A.: 1980, Ap.J., 242, 1056

Lada, C.J., Thronson, H.A., Smith, H.A., Harper, D.A., Keene, J., Loewenstein, R.F., and Smith, J.: 1981, Ap.J., 251, L91

Sellgren, C.: 1983, Ph.D. Thesis

Smith, H.A., Thronson, H.A., Lada, C.J., Harper, D.A., Loewenstein, R.F. and Smith, J.: 1982, Ap.J., 258, 170

TABLE 1
IRAS FLUXES AND DUST TEMPERATURES[a,b]

	12 μm	25 μm	60 μm	100 μm	T_H	T_L	L_H	L_H
	(Jy)				(K)		($L_\odot$)	
Outer Rim (area$\approx 1.8\times10^{-4}$ sr)	47.5	50.7	318	1702	292	25.5	81	312
Inner Limb (area $\approx 5.1\times10^{-5}$ sr)	33.3	48.7	292	1607	251	25.3	61	296
Central Core (area $\approx 7.8\times10^{-6}$ sr)	7.1	18.9	203	475	200	33.0	18	87

[a] IRAS color corrected fluxes, assumming for the correction a T≈200K blackbody (β=0) for the 12 and 25 μm fluxes, and a β=1 emissivity dependence to the 60 and 100 μm emission. The corrected raw data points were then fit to β=0 and 1 blackbodies, respectively, and the corrected fluxes and derived temperatures and luminosities listed here.

[b] We have estimated the 3σ error bars as ±10% in the 12 and 25 μm data, and ±30% in the 60 and 100 μm data. These error bars reflect both uncertainties in the raw data, the color correction values, the two temperature fits, and possible variations in β.